Journal of Computer-Aided Molecular Design, 7 (1993) 699–720
ESCOM

J-CAMD 216

A molecular mechanics study of the effect of substitution in position 1 on the conformational space of the oxytocin/vasopressin ring

Monika Tarnowska[a], Adam Liwo[a,*], Mark D. Shenderovich[b], Inta Liepiņa[b], Alexander A. Golbraikh[b], Zbigniew Grzonka[a] and Anna Tempczyk[a]

[a]*Department of Chemistry, University of Gdańsk, ul. Sobieskiego 18, 80-952 Gdańsk, Poland*
[b]*Institute of Organic Synthesis, Latvian Academy of Sciences, Aizkraukles 21, LV 1006 Riga, Latvia*

Received 18 January 1993
Accepted 19 March 1993

Key words: Conformational energy calculations; Disulfide-bridge conformation; Oxytocin and vasopressin analogs; Structure–activity relationship

SUMMARY

The effect of the substitution in position 1 on the low-energy conformations of the oxytocin/vasopressin 20-membered ring was investigated by means of molecular mechanics. Three representative substitutions were considered: (β′-mercapto-β,β-dimethyl)propionic acid (Dmp), (β′-mercapto-β,β-cyclopentamethylene)propionic acid (Cpp), both forming strong antagonists, and (α,α-dimethyl-β-mercapto)propionic acid (α-Dmp), forming analogs of strongly reduced biological activity, with the β-mercaptopropionic (Mpa) residue taken as reference. Both ECEPP/2 (rigid valence geometry) and AMBER (flexible valence geometry) force fields were employed in the calculations. Three basic types of backbone conformations were taken into account which are distinguished by the type of β-turn at residues 3 and 4: β1/βIII, βII, and βI′/βIII′, all types containing one or two intra-annular hydrogen bonds. The allowed (ring-closed) disulfide- bridge conformations were searched by an algorithm formulated in terms of scanning the disulfide-bridge torsional angle C^{β}–S–S–C^{β}. The ECEPP/2 and AMBER energies of the obtained conformations were found to be in reasonable agreement. Two of the low-energy conformers of the [Mpa^1]-compound agreed very well with the cyclic part of the two conformers found in the crystal structure of [Mpa^1]-oxytocin. An analysis of the effect of β-substitution on relative energies showed that the conformations with the N–C′–CH_2–CH_2 (ψ'_1) and C′–CH_2–CH_2–S (χ'_1) angles of the first residue around (−100°, 60°) and (100°, −60°) are not affected; this in most cases implies a left-handed disulfide bridge. In the case of α-substitution the allowed values of ψ'_1 are close to ± 60°. This requirement, being in contradiction to the one concerning β-substitution, could explain the very low biological activity of the α-substituted analogs. The conformational preferences of substituted compounds can largely be explained by the analysis of local interactions within the first residue. Based on the selection of the conformations which are low in energy for both the reference and β-substituted compounds, two distinct types of possible binding conformations were proposed, the first one being similar to the crystal conformer with a left-handed disulfide bridge, the second one having a right-handed bridge, but a geometry different from that of the crystal conformer with the right-handed bridge. The first type of disulfide-bridge

*To whom correspondence should be addressed.

arrangement is equally favorable for both βI/βIII and βII types of backbone structure, while the second one is allowed only for the βII type of backbone. No conformation of the βI′/βIII′ type has a low enough energy to be considered as a possible binding conformation for all of the active compounds studied in this work.

INTRODUCTION

Oxytocin (OT) and vasopressin (VP) are important hormones in the functioning of all vertebrates. They induce four primary biological actions: uterine contraction, milk ejection, pressor, and antidiuresis, the first two being more characteristic of oxytocin and the latter two of vasopressin. They have the following primary structure:

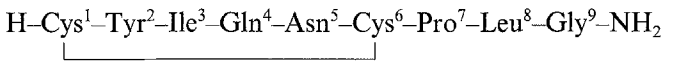

oxytocin

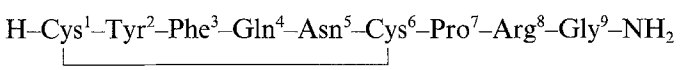

vasopressin

The difference in the type of activity exhibited by a particular hormone (or analog) is connected with the kind of amino acid residues occupying positions 3 and 8 [1]. The compounds exhibiting activities antagonistic to those of the parent hormones are also important from the medical point of view [1].

A number of effective oxytocin and vasopressin antagonists have been obtained by attaching bulky substituents to the β-carbon of the amino acid residue in position 1 [1]. Hruby et al. [2] postulated that this antagonistic activity is connected with impairing the conformational changes of the disulfide bridge, one type of disulfide-bridge chirality becoming strongly preferred to the second one on substitution. In our previous paper on the conformational analysis of (β′-mercapto-β,β-cyclopentamethylene)propionic acid-1-sarcosine-7 arginine vasopressin ([Cpp¹,Sar⁷,Arg⁸]-VP) [3], we found that ring conformations with left-handed disulfide-bridge chirality (i.e. C_1^β–S–S–C_6^β dihedral-angle values about −90°) are preferred for a [Cpp¹]-substituted ring, which conforms with the hypothesis of Hruby et al. [2]. However, in order to draw more convincing conclusions regarding the influence of substitution in position 1 on the conformational mobility of the disulfide bridge, the set of low-energy conformations of differently substituted analogs should be compared.

Recently [4] we have carried out the Free–Wilson decomposition of the activities characteristic of oxytocin and vasopressin analogs which resulted in the numerical values of the activity contributions of separate amino acid residues. In particular, the contributions of the side chains in position 1 appear to be connected with the bulkiness of the substituent(s) attached to the β-carbon, as shown in Table 1.

According to these data, three residues in position 1 of gradually increasing steric bulk have been chosen for comparative conformational study: β-mercaptopropionic acid (Mpa), (β′-mercapto-β,β-dimethyl)propionic acid (Dmp), and (β′-mercapto-β,β-cyclopentamethylene)propionic acid (Cpp), of which Mpa can be considered as a reference residue, owing to the absence of any

β-carbon substituent. The bulkiest Cpp residue is known to give the best antagonists in general [1]. In addition, we also examined the effect of shifting the substituents to position α – the (α,α-dimethyl-β-mercapto)propionic acid (α-Dmp) which, according to Table 1, results in remarkable diminishing of the affinity towards the receptors (no agonistic and weak antagonistic activity). Only main-chain conformations of the cyclic part were considered and therefore model compounds were chosen that had side chains (except for those of the first and the sixth residue) modeled by single interaction sites (vide infra).

METHODS

The force fields used in molecular-mechanics calculations

As in our earlier study of [Cpp[1],Sar[7],Arg[8]]VP [3] we carried out the conformational calculations using both ECEPP/2 (rigid valence geometry) [5,6] and AMBER (flexible valence geometry) [7] potential functions. Although, of the two force fields, ECEPP/2 was shown to represent better the energy surfaces and properties of model peptides [8], the AMBER force field also has some advantages (e.g. better parametrized electrostatic-interaction energy) [7]. Moreover, the use of rigid valence geometry often results in trapping of the molecule in a region of the conformational space of relatively high energy during energy minimization, due to restricted possibility of motion. Conversely, when a flexible-valence-geometry force field is applied, the molecule can find a way out of this region and, consequently, minimization can lead to a conformation remarkably lower in energy. The latter can be used as a starting point for another run in the rigid-valence-geometry force field. On the other hand, a greater number of variables in the case of flexible-

TABLE 1
SELECTED SEGMENT CONTRIBUTIONS IN POSITION 1 TO THE AGONISTIC (LEFT) AND ANTAGONISTIC (RIGHT) ACTIVITIES CHARACTERISTIC OF NEUROHYPOPHYSEAL HORMONES (VALUES FROM Ref. 4)

Amino acid residue[a]	Activity[b]					
	Uterotonic		Pressor		Antidiuretic	
Relative to:	Cys	Cpp	Cys	Cpp	Cys	Cpp
Mpa	0.23	−0.14	−0.08	−1.15	0.26	–
Dmp	−1.71	−0.12	–	−0.18	−0.74	–
Dep	–	0.08	–	0.06	–	–
Cpp	–	0.00	−0.75	0.00	–	0.00
Cys	–	−0.59	–	−1.19	–	0.17
Pen	–	−0.38	–	−0.59	–	–
α-Dmp	–	−0.74	–	–	–	–

[a] *Abbreviations:* Mpa = β-mercaptopropionic acid; Dmp = (β′-mercapto-β,β-dimethyl)propionic acid; Dep = (β′-mercapto-β,β-diethyl)propionic acid; Cpp = (β′-mercapto-β,β-cyclopentamethylene)propionic acid; Pen = penicillamine; α-DMP = (α,α-dimethyl-β-mercapto)propionic acid.

[b] The numerical values of activity contributions presented here indicate the change of activity of a reference compound, i.e. with such a substituent in position 1 as in the heading of the corresponding column, on the respective substitution. Antagonistic activity is measured in pA_2 units, while the decimal logarithm of agonistic activity was considered [4].

valence-geometry treatment can result in numerical problems, e.g. obtaining false minima (see also a recent paper by Palmer and Scheraga [9] for more discussion about the motivation for using the rigid- or flexible-valence-geometry). For these reasons, in this study we performed calculations using both force fields, assigning, however, a greater weight to the ECEPP/2 results.

Because the aim of this work was the comparative investigation of the cyclic-moiety conformations for the series of oxytocin/vasopressin analogs substituted in position 1, the simplest possible models were chosen for the side chains in positions 2–5, that is, methyl groups in the ECEPP/2 force-field calculations, or united side chains (i.e. pseudo-atoms of appropriate size) [3,10] in the AMBER force-field calculations. Therefore, no additional degrees of freedom due to side-chain internal rotation had to be taken into account which reduced the number of minima on the energy surfaces of the compounds studied. Such an approach was already implemented in other authors' [11,12], as well as in our [3,10] previous works on the oxytocin/vasopressin cyclic part and was proved to give energy relations qualitatively similar to those of the conformations of the oxytocin/vasopressin ring with complete side chains in the lowest-energy conformations [3,10]. The C-terminal cysteine was terminated by the *N,N*-dimethylamino group which simulated the steric influence of an *N*-methylene substituent in position 7. The full sequences of the model compounds studied are the following:

$$X^1\text{–}\,Ala^2\text{–}Ala^3\text{–}Ala^4\text{–}Ala^5\text{–}Cys^6\text{–}NMe_2$$

for the ECEPP/2 force field and

$$X^1\text{–}\,Tyr^{*2}\text{–}Ile/Phe^{*3}\text{–}Gln^{*4}\text{–}\,Asn^{*5}\text{–}\,Cys^6\text{–}NMe_2$$

for the AMBER force field,
where X = Mpa, Dmp, Cpp or α-Dmp, and asterisks indicate united side chains. It should be noted that the force-field parameters for the Ile and Phe united side chains are identical, as found in an earlier study [10]. Hence common model compounds were considered for oxytocin and vasopressin in the AMBER force field.

As in our earlier studies [3,10], the use of bulkier side-chain models in the AMBER force field was motivated by the fact that flexible valence geometry, being less restrictive, could lead to conformations that are too collapsed, if the poly-alanine model were implemented. However, the final AMBER conformations were also minimized using the poly-alanine model of the chain, in order to check the influence of side-chain dimensions on the results.

The united-atom approximation (i.e. all aliphatic hydrogens fused with carbons to which they are attached) was extensively applied in calculations with the AMBER potentials. However, the explicit treatment of α-hydrogens in the ECEPP/2 force field is required in order to obtain a reasonable representation of local interactions. If these atoms are removed, additional torsional terms, such as in UNICEPP [13], must be introduced. Because for the neighborhood of the disulfide bridge the local interactions can also be important, we left explicit hydrogens on the methylene groups of the bridge. The methyl groups of alanine residues and the methyl and methylene groups of the β-carbon substituents of Dmp and Cpp, as well as the α-carbon methyl groups of α-Dmp were considered as united atoms with UNICEPP parameters [13]. Such a

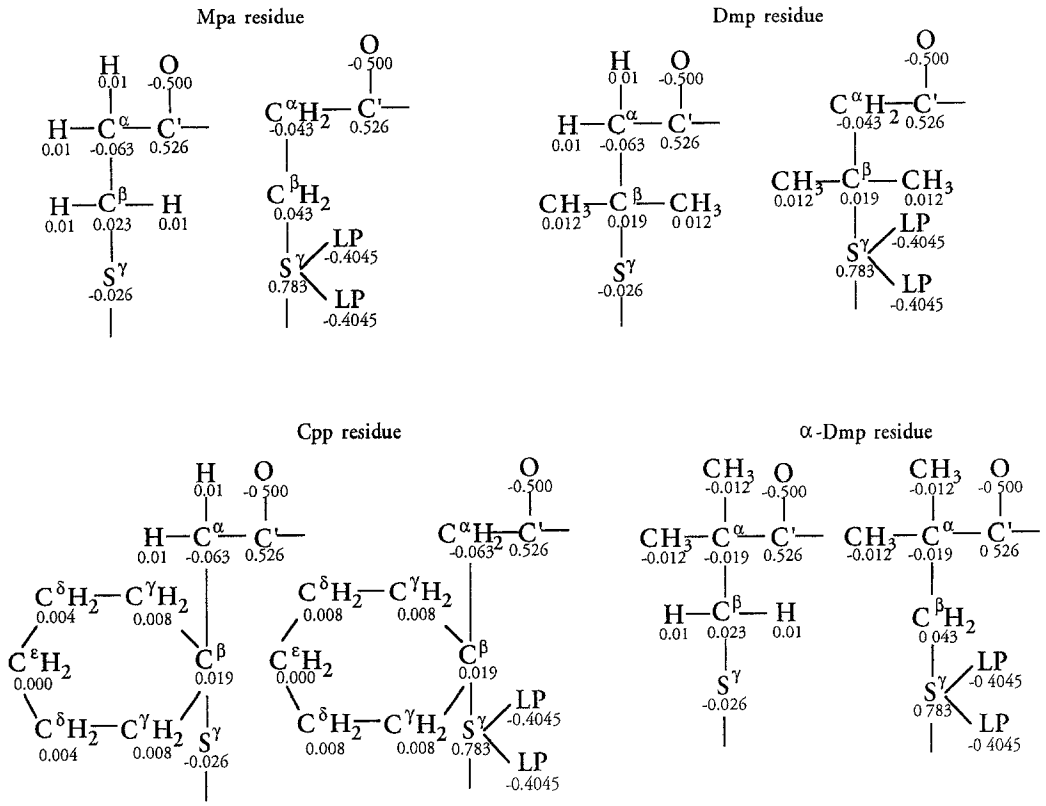

Fig. 1. The charges on the nonstandard residues used in ECEPP/2 (left) and AMBER (right) force-field calculations.

combined approach was proved to produce the energy map of a blocked L-alanine residue practically indistinguishable from the map resulting from all-atom ECEPP/2 calculations, in which the methyl group of the alanine side chain and those of the blocking groups had explicit hydrogens (M.D. Shenderovich, unpublished observations). The chair conformation of the cyclohexyl ring of the Cpp residue was chosen, the sulfur atom and α-methylene group being attached as the axial and equatorial substituent respectively (the Cpp_{ax} residue). The reverse arrangement (the Cpp_{eq} residue) was also considered, but it resulted in a substantially higher conformational energy in almost all cases, due to greater nonbonded repulsion.

The atomic charges of the Mpa, Dmp, Cpp, and α-Dmp side chains (Fig. 1) were estimated based on a CNDO/2D population analysis and were used with both the ECEPP/2 and AMBER force fields. For other residues and blocking groups standard ECEPP charges [5] and a dielectric constant $\varepsilon = 4.0$ [8] were used with the ECEPP/2 potential functions. For the AMBER force-field calculations we used the charges as described in our earlier study of 1-substituted vasopressin analogs [10], and a distance-dependent dielectric constant $\varepsilon = r_{ij}$.

Standard ECEPP/2 nonbonded, hydrogen-bond, and torsional parameters [5,6] were used in the first force field, while AMBER standard nonbonded, hydrogen-bond, torsional, bond, and bond-angle constants [7] supplemented with the values obtained in our earlier study [10] were used in the second force field.

In the ECEPP/2 force field a set of penalty functions was employed to achieve the disulfide-bridge closure with standard geometry: d(S–S) = 2.04 Å, $\alpha(C^{\beta}–S–S) = 104°$ and ($C^{\beta}–S–S–C^{\beta}$) dihedral-angle values near ± 90°. First a force constant of 100.0 kcal/(mol Å^2) was imposed on interatomic distances d(S–S), $d(C_1^{\beta}...S_6^{\gamma})$, and $d(C_6^{\beta}...S_1^{\gamma})$, while a constant of 10.0 kcal/(mol Å^2) was imposed on the distance $d(C_1^{\beta}...C_6^{\beta})$. At the final stage of energy minimization the force constant for the first three distances was increased to 1000.0 kcal/(mol Å^2) in order to avoid large deviations from the standard geometry. Owing to the use of flexible valence geometry, there was no disulfide-bridge closure problem to be solved in AMBER force-field calculations.

The ECEPP/2 energy maps of the C-terminally blocked first residues of the compounds studied, X-NHMe, where X represents Mpa, Cpp, Dmp, or α-Dmp, were calculated on a uniform square grid ($-180° \leq \psi < 180°$) × ($-180° \leq \chi' < 180°$) with steps of 15° on both axes.

An algorithm for the search of the conformational space accessible for the disulfide bridge

Because the substitutions considered in this study influence directly the side-chain conformation in position 1, it is very important to carry out an extensive search of possible disulfide-bridge conformations allowed for each backbone conformation. This means that all conformations of the bridge must be sought which satisfy (i) the bond-length constraint (2.04 Å) at the S–S bond, (ii) two bond-angle constraints (104°) at the $C^{\alpha}–C^{\beta}–S$ atoms, and (iii) the dihedral-angle constraint (± 90°) at the $C^{\beta}–S–S–C^{\beta}$ atoms. While constraints (i) and (ii) can be regarded as strict, the energy required to distort the $C^{\beta}–S–S–C^{\beta}$ dihedral angle from ± 90° (the optimum values) is comparatively low [5,7] and, therefore, the conformations in the neighborhood of these two dihedral-angle values must also be considered. This problem could be treated, although not in a straightforward way, by the well-known Gō–Scheraga algorithm [9,14–17]. However, in order to handle this specific case, we developed a ring-closure algorithm that is specially designed for disulfide bridges and is formulated in such a way that the single dihedral angle to be scanned is the $C^{\beta}–S–S–C^{\beta}$ angle.

Let us take our model of the OT/VP cyclic part and assume that the backbone (which extends from $C^{\alpha}(X^1)$ to $C^{\alpha}(Cys^6)$) has a fixed conformation. In this case only the side chains of residues 1 and 6 and the blocking group can move. Thus, the disulfide-bridge closure problem could be formulated as the solution of four equations, which include constraints (i), (ii), and (iii), in four unknowns, the latter being the disulfide-bridge dihedral angles ω_1 and ω_2 defined in Fig. 2, and the angles χ'_1 ($C'_1–C_1^{\alpha}–C_1^{\beta}–C_1^{\gamma}$) and χ_6^1 of the terminal amino acid residues. The following relations hold between ω_1, ω_2 and the backbone dihedral angles of Cys^1 and Cys^6:

$$\omega_1 = \psi'_1$$

$$\omega_2 = \phi_6 - 120°$$

where ψ_1 is the dihedral angle defined by atoms $C_1^{\beta}–C_1^{\alpha}–C'_1–N_2$.

Such a system of equations could be solved by any relevant numerical method, using e.g. Monte Carlo methods to explore the solution space. However, if we can reduce the problem to solving one equation in a single unknown, scanning of the solution space becomes much easier. The first reason for this is the reduction of the dimensionality of the problem. The second reason is that each solution can easily be bracketed (i.e. we can determine and subsequently narrow down the interval which includes it).

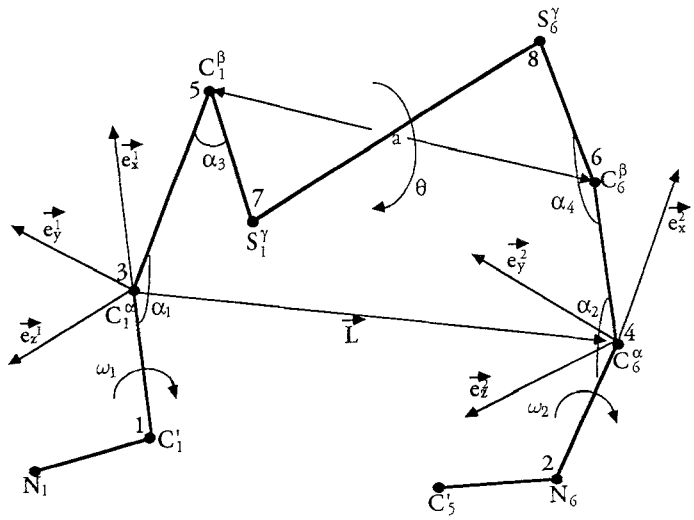

Fig. 2. Definition of the disulfide-bridge geometry and designation used in the disulfide-bridge closure algorithm.

Let us consider the problem illustrated in Fig. 2. The variables defining the movement are now the dihedral angles ω_1 and ω_2 and the angle θ defining the rotation of the rigid (i.e. with a fixed value of the C^β–S–S–C^β dihedral angle) disulfide bridge about the $C_1^\beta \ldots C_6^\beta$ axis. This angle is defined to be zero when the atom S_1^γ lies in the plane defined by the atoms C_1^α, C_1^β, and C_6^β, on the same side of the $C_1^\beta \ldots C_6^\beta$ axis as C_1^α. This angle is positive when the bridge is rotated clockwise when looking from C_1^β to C_6^β (Fig. 2). We can now write a system of three equations for the $C_1^\alpha \ldots C_6^\alpha$ distance and the C_1^α–C_1^β–S_1^γ and C_6^α–C_6^β–S_6^γ valence angles, respectively:

$$\|r_6 - r_5\| = a \tag{1a}$$

$$\frac{(r_3 - r_5) \cdot (r_7 - r_5)}{d_3 d_5} = \cos \alpha_3 \tag{1b}$$

$$\frac{(r_4 - r_6) \cdot (r_8 - r_6)}{d_4 d_6} = \cos \alpha_4 \tag{1c}$$

where the bond lengths $d_3 = \|r_5 - r_3\|$, $d_4 = \|r_6 - r_4\|$, $d_5 = \|r_7 - r_5\|$, and $d_6 = \|r_s - r_6\|$ are all fixed and known.

Since the distance α is a function of ω_1 and ω_2 only, following Eq. 1a we can express ω_2 as a function of ω_1. This can be achieved as follows. Let the reference systems connected with C_1^α and C_6^α be defined as in Fig. 2, the x axes being chosen along the vectors C_1'–C_1^α and N_6–C_6^α, respectively, while the xy planes are defined by the atoms C_1^β–C_1^α–C_1' and C_6^β–C_6^α–N_6. The Cartesian coordinates of atoms C_1^β and C_6^β in these local systems are defined by Eq. 2:

$$r_3' = \begin{pmatrix} d_3 \cos \alpha_1 \\ d_3 \sin \alpha_1 \cos \omega_1 \\ d_3 \sin \alpha_1 \sin \omega_1 \end{pmatrix} \qquad r_4' = \begin{pmatrix} d_4 \cos \alpha_2 \\ d_4 \sin \alpha_2 \cos \omega_2 \\ d_4 \sin \alpha_2 \sin \omega_2 \end{pmatrix} \tag{2}$$

The positions of these atoms in a global reference system, r_3 and r_4, can be calculated by using the following formulas:

$$r_3 = \mathbf{E}_1^T r'_3 \quad r_4 = \mathbf{E}_2^T r'_4 + \mathbf{L} \tag{3}$$

where $\mathbf{E}_1$ and $\mathbf{E}_2$ are the matrices of the local reference systems:

$$\mathbf{E}_1 = \begin{pmatrix} e_{x1}^1 & e_{x2}^1 & e_{x3}^1 \\ e_{y1}^1 & e_{y2}^1 & e_{y3}^1 \\ e_{z1}^1 & e_{z2}^1 & e_{z3}^1 \end{pmatrix} \qquad \mathbf{E}_2 = \begin{pmatrix} e_{x1}^2 & e_{x2}^2 & e_{x3}^2 \\ e_{y1}^2 & e_{y2}^2 & e_{y3}^2 \\ e_{z1}^2 & e_{z2}^2 & e_{z3}^2 \end{pmatrix}$$

and $\mathbf{L}$ is the vector pointing from C_α^1 to C_α^6. Thus Eq. 1a can be rearranged to give Eq. 4:

$$\begin{aligned} a^2 &= \|\mathbf{E}_2^T r'_4 - \mathbf{E}_1^T r'_3 + \mathbf{L}\|^2 \\ &= d_3^2 + d_4^2 + L^2 - 2(r'^T_3 \mathbf{E}_1 \mathbf{E}_2^T r'_4 - \mathbf{L}^T \mathbf{E}_2^T r'_4 + \mathbf{L}^T \mathbf{E}_1^T r'_3) \\ &= d_3^2 + d_4^2 + L^2 - 2(r'^T_3 \mathbf{Q} r'_4 + \mathbf{L}^T \mathbf{E}_1^T r'_3 + \mathbf{L}^T \mathbf{E}_2^T r'_4) \end{aligned} \tag{4}$$

where $L = \|\mathbf{L}\|$ and $\mathbf{Q} = d_3 d_4 \mathbf{E}_1 \mathbf{E}_2^T$.

After performing all the necessary operations, Eq. 4 can be expressed as Eq. 5:

$$\begin{aligned} &q_{11} \cos\alpha_1 \cos\alpha_2 + q_{12} \cos\alpha_1 \sin\alpha_2 \cos\omega_2 + q_{13} \cos\alpha_1 \sin\alpha_2 \sin\omega_2 + \\ &q_{21} \sin\alpha_1 \cos\alpha_2 \cos\omega_1 + q_{31} \sin\alpha_1 \cos\alpha_2 \sin\omega_1 + q_{22} \sin\alpha_1 \sin\alpha_2 \cos\omega_1 \cos\omega_2 + \\ &q_{23} \sin\alpha_1 \sin\alpha_2 \cos\omega_1 \sin\omega_2 + q_{32} \sin\alpha_1 \sin\alpha_2 \sin\omega_1 \cos\omega_2 + \\ &q_{33} \sin\alpha_1 \sin\alpha_2 \sin\omega_1 \sin\omega_2 + L_{1x} \cos\alpha_1 + L_{1y} \sin\alpha_1 \cos\omega_1 + \\ &L_{1z} \sin\alpha_1 \sin\omega_1 - L_{2x} \cos\alpha_2 - L_{2y} \sin\alpha_2 \cos\omega_2 - L_{2z} \sin\alpha_2 \sin\omega_2 + \\ &\tfrac{1}{2}(a^2 - L^2 - d_3^2 - d_4^2) = 0 \end{aligned} \tag{5}$$

where $\mathbf{L}_1 = d_3 \mathbf{E}_1 \mathbf{L}$, $\mathbf{L}_2 = d_4 \mathbf{E}_2 \mathbf{L}$, and q_{ij} are the elements of the matrix $\mathbf{Q}$.

Grouping all the terms with ω_2 we obtain Eq. 6:

$$A \sin\omega_2 + B \cos\omega_2 + C = 0 \tag{6}$$

with

$$\begin{aligned} A &= q_{13} \cos\alpha_1 \sin\alpha_2 + q_{23} \sin\alpha_1 \sin\alpha_2 \cos\omega_1 + q_{33} \sin\alpha_1 \sin\alpha_2 \sin\omega_1 - L_{2z} \sin\alpha_2 \\ B &= q_{12} \cos\alpha_1 \sin\alpha_2 + q_{22} \sin\alpha_1 \sin\alpha_2 \cos\omega_1 + q_{32} \sin\alpha_1 \sin\alpha_2 \sin\omega_1 - L_{2y} \sin\alpha_2 \\ C &= q_{11} \cos\alpha_1 \cos\alpha_2 + q_{21} \sin\alpha_1 \cos\alpha_2 \cos\omega_1 + q_{31} \sin\alpha_1 \cos\alpha_2 \sin\omega_1 + L_{1x} \cos\alpha_1 + \\ &\quad L_{1y} \sin\alpha_1 \cos\omega_1 + L_{1z} \sin\alpha_1 \sin\omega_1 + \tfrac{1}{2}(a^2 - L^2 - d_3^2 - d_4^2) \end{aligned}$$

This equation can be solved analytically for $\tan(\omega_2/2)$ giving in general two solutions:

$$\tan\frac{\omega_2^{12}}{2} = \frac{-B \mp (A^2 + B^2 - C^2)^{1/2}}{C - A} \tag{7}$$

These expressions make sense, if the determinant of the quadratic equation, $A^2 + B^2 - C^2$, is non-negative. To find the ω_1 interval for which ω_2 values can be calculated, the sign of the determinant must be scanned. This is equivalent to solving a fourth-power inequality in $\tan(\omega_1/2)$. The coefficients of this inequality can be obtained from the expressions for A, B, and C. Because the resulting expressions are lengthy and not especially interesting, they are not presented here.

Let us now turn to constructing the final equation. To develop Eqs. 1b and 1c let us first calculate the coordinates of atoms C_1^α, C_6^α, C_1^β, C_6^β, S_1^γ, and S_6^γ. Let the reference system be defined by vectors C_1^β–C_6^β and C_1^α–C_1^β. The expressions for Cartesian coordinates are as follows:

$$r_3 = \begin{pmatrix} d_3 \cos \xi_1 \\ -d_3 \sin \xi_1 \\ 0 \end{pmatrix} \qquad r_5 = \begin{pmatrix} 0 \\ 0 \\ 0 \end{pmatrix} \qquad r_7 = \begin{pmatrix} d_5 \cos \beta_1 \\ -d_5 \sin \beta_1 \cos \theta \\ -d_5 \sin \beta_1 \sin \theta \end{pmatrix}$$

$$r_4 = \begin{pmatrix} -d_4 \cos \xi_2 + a \\ -d_4 \sin \xi_2 \cos \delta \\ -d_4 \sin \xi_2 \sin \delta \end{pmatrix} \qquad r_6 = \begin{pmatrix} a \\ 0 \\ 0 \end{pmatrix} \qquad r_8 = \begin{pmatrix} -d_6 \cos \beta_2 + a \\ -d_6 \sin \beta_2 \cos (\theta+\varepsilon) \\ -d_6 \sin \beta_2 \sin (\theta+\varepsilon) \end{pmatrix}$$

where ξ_1, ξ_2, β_1, and β_2 are the angles between atoms C_1^α–C_1^β–C_6^β, C_1^β–C_6^β–C_6^α, C_6^β–C_1^β–S_1^γ, and S_6^γ–C_6^β–C_6^α, respectively, δ is the torsion angle defined by atoms C_1^α–C_1^β–C_6^β–C_6^α, and ε is the internal bridge torsion angle defined by atoms S_1^γ–C_1^β–C_6^β–S_6^γ.

Then Eqs. 1b and 1c can be written as Eqs. 8a and 8b:

$$\eta_1 = \cos \xi_1 \cos \beta_1 + \sin \xi_1 \sin \beta_1 \cos \theta = \cos \alpha_3 \tag{8a}$$

$$\eta_2 = \cos \xi_2 \cos \beta_2 + \sin \xi_2 \sin \beta_2 \cos \delta \cos(\theta + \varepsilon) + \sin \xi_2 \sin \beta_2 \sin \delta \sin(\theta + \varepsilon) = \cos \alpha_5 \tag{8b}$$

Obviously, the angles ξ_1, ξ_2, β_1, and β_2 are dependent on ω_1 and ω_2. Since ω_2 can be treated as a biunivocal function of ω_1 (Eq. 7), so can these angles and, consequently, the expressions for η_1 and η_2 (Eqs. 8a and 8b). In order to obtain the final equation in ω_1 only, let us determine $\cos \theta$ from Eq. 8a which results in Eq. 9a. After inserting Eq. 9a into Eq. 8b and performing the necessary arithmetic operations we obtain Eq. 9b which is exactly the desired equation in a single unknown ω_1:

$$\cos \theta = \frac{\eta_1 - \cos \xi_1 \cos \beta_1}{\sin \xi_1 \sin \beta_1} \tag{9a}$$

$$[(\eta_2 - \cos \beta_2 \cos \xi_2) \sin \beta_1 \sin \xi_1]^2 + [(\eta_1 - \cos \beta_1 \cos \xi_1) \sin \beta_2 \sin \xi_2]^2 -$$
$$2 (\eta_1 - \cos \beta_1 \cos \xi_1) (\eta_2 - \cos \beta_2 \cos \xi_2) \sin \beta_1 \sin \xi_1 \sin \beta_2 \sin \xi_2 \cos (\varepsilon - \delta) = 0 \tag{9b}$$

To find the solutions of this equation the whole domain allowed for ω_1 must be scanned with a dense enough grid and all intervals examined in which the left side of Eq. 9b changes its sign. In this work a grid size of 2° was applied. After finding the desired intervals the solution of Eq. 9b was calculated in each of them by means of the *regula falsi* method [18]. It must be noted at this point that because ω_2 is a biunivocal function of ω_1 there are two families of solutions.

For each value of ω_1 thus found, we can calculate the angles ξ_1, ξ_2, β_1, and β_2 and find cos θ following Eq. 9a. This will give two distinct values of the angle θ, of which one only, in general, or both, in some special cases, satisfy both Eqs. 8a and 8b. This should be checked and the right value(s) of θ selected. Having the values of ω_1, ω_2 and θ we can calculate the Cartesian coordinates of atoms C_1^{α}, C_6^{α}, C_1^{β}, C_6^{β}, S_1^{γ}, and S_6^{γ} as shown above and, finally, the dihedral angles ξ_1^1 and ξ_1^6 of the terminal cysteines which completes the solution of the ring-closure problem.

The algorithm described was written in TURBO Pascal and implemented on an IBM PC AT computer, as part of a multi-functional program GEOM developed in our laboratory.

RESULTS AND DISCUSSION

The procedure of calculations

As was shown in our previous paper [3], the backbone conformations of the vasopressin 20-membered ring which are both low in energy and consistent with NMR data contain a β-turn at the residues Phe[3]–Gln[4], stabilized by at least one of the two intramolecular hydrogen bonds between Tyr[2](NH)...Asn[5](CO) and Asn[5](NH)...Tyr[2](CO). The same type of backbone conformation of the cyclic part of oxytocin was found in a recent NMR and restrained molecular dynamics study by Bhaskaran et al. [19]. We have shown that the classification based upon the type of β-turn gives three distinct families of backbone structures: βI/βIII, βII, and βI′/βIII′ [3] (the βII′-turn implies a nearly C_{ax}^7 conformation at the third residue which is sterically forbidden). The βI/βIII and βI′/βIII′ turns were considered as common types of structures, because they form continuous clusters in the conformational space [20] with no clear boundary separating the βI-type turns from the βIII-type turns or the βI′-type turns from the βIII′-type turns. Their energetic preference depends on the force field applied in calculations. Conformations βIII and βIII′ are usually lower in energy in the ECEPP/2 force field, while conformations βI and βI′ are lower in energy in the AMBER force field, probably because they lead to stronger electrostatic interactions, which play a much greater role in the AMBER than in the ECEPP/2 force field [3]. For reasons pointed out above we thought it reasonable to restrict the present study to these three types of backbone conformations only, i.e. βI/βIII, βII, and βI′/βIII′.

The starting backbone structures in both force fields contained βI-, βIII-, βI′-, βIII′-, and βII-type conformations; however in the case of the AMBER force field single energy minimizations starting from the βIII- and βIII′-turns always converged to the βI- and βI′-turns, respectively.

The disulfide-bridge geometry was examined for each type of backbone conformation by scanning the C_1^{β}–S–S–C_6^{β} dihedral angle in the intervals $[-110°,-70°] \cup [70°,110°]$ (i.e. around $\pm$ 90°) with a grid size of 2° and using the algorithm described in the previous section to solve the bridge-closure equations. The maximum number of solutions found for a given backbone conformation and for a given value of the disulfide-bridge dihedral angle was usually eight, though up to twelve solutions were obtained for the βIII-type backbone conformation.

For both intervals defined above, the conformations of the bridge were chosen, corresponding to that value of the C_1^{β}–S–S–C_6^{β} dihedral angle for which the greatest number of bridge-closure solutions were obtained. A total of about 100 starting conformations were generated for all of the types of backbone and the two possible types of disulfide-bridge chirality. These conformations were taken as starting points for both the ECEPP/2 and AMBER force-field calculations on the

TABLE 2
RELATIVE ENERGIES OF THE CONFORMATIONS OF [Mpa^1]-, [Dmp^1]-, [Cpp^1]-, AND [α-Dmp^1]-SUBSTITUTED OT/VP RINGS AS CALCULATED IN THE ECEPP/2 (LEFT) AND AMBER (RIGHT) FORCE FIELDS

Type of conformation[a]	Bridge chirality	Angles ψ'_1, χ'_1 (deg)[a]		Relative energy (kcal/mol)							
				Mpa^1		Dmp^1		Cpp^1		α-Dmp^1	
βIII (βI)											
1[d]	L	−110	60	0.0	0.0	0.0	0.0	0.0	0.0	10.2	3.5
2[e]	R	−90	140	0.1	5.1	7.0	6.6	13.4	6.4	5.8	5.6
3	L	−60	−50	1.6	0.3	9.3	–[b]	7.5	–[b]	0.0	0.0
4	L	−90	60	3.4	10.0	2.8	–[b]	3.1	–[b]	11.6	–[b]
5	R	−120	50	5.6	8.3	3.3	7.8	1.9	8.4	23.4	12.7
6	R	−60	−50	5.8	5.5	8.5	12.2	7.1	[5.8][c]	4.0	5.9
7	L	80	−140	6.4	–	10.8	–	11.6	–	24.9	–
8	R	80	−140	–	7.0	–	8.4	–	8.0	–	8.9
9	L	−130	60	–[b]	4.7	–[b]	5.7	–[b]	5.9	–[b]	[0.0][c]
βII											
1[f]	L	−130	60	0.8	0.4	1.1	0.4	0.6	0.4	13.2	4.8
2	L	80	−170	1.3	5.9	8.5	7.4	15.9	7.0	6.0	7.3
3	R	60	60	2.0	4.1	7.5	5.5	7.2	8.5	0.9	4.8
4	R	120	−60	2.6	2.8	4.8	4.8	8.6	5.0	21.3	4.9
5[g]	R	−110	150	2.7	5.3	10.4	6.0	13.3	5.8	8.5	6.1
6	R	140	−60	3.5	4.7	3.2	5.4	1.8	5.6	17.7	8.1
7	R	90	−150	3.6	9.4	10.1	11.8	11.1	11.9	16.3	10.9
8	R	100	−70	3.8	–[b]	5.4	–[b]	7.4	–[b]	7.7	–[b]
9	L	−90	60	4.3	8.2	4.0	8.6	5.1	8.8	12.5	12.2
10[h]	L	−70	170	4.4	8.0	9.7	8.2	8.7	7.8	12.7	10.3
11	L	80	−170	6.1	–[b]	7.5	–[b]	8.6	–[b]	9.2	–[b]
12	R	80	−170	7.2	8.6	14.1	9.3	12.9	7.7	14.1	12.1
13	R	−120	60	9.0	8.2	6.5	7.6	3.2	8.1	26.8	12.9
14	L	−100	60	9.2	7.6	6.5	8.2	8.1	9.6	13.1	9.5
15	L	−130	70	–[b]	6.9	–[b]	8.8	–[b]	8.9	–[b]	11.9
βIII′ (βI′)											
1′	R	−70	−170	2.6	8.5	4.8	[2.7][c]	7.3	[3.5][c]	4.5	5.2
2	L	−100	70	6.6	5.4	10.1	6.1	9.7	7.7	12.2	5.7
3	R	−140	60	7.1	7.0	6.2	6.6	4.3	7.0	24.6	12.1
4	R	70	180	8.0	8.7	7.6	[4.4][c]	6.4	7.8	7.9	[5.9][c]
5	R	−170	170	9.4	4.2	16.6	[3.3][c]	19.3	[3.4][c]	18.7	[5.2][c]
6	R	130	−60	–[b]	5.5	–[b]	5.5	–[b]	5.7	–[b]	8.8

[a] Dihedral angles ψ'_1, χ'_1 (comprising atoms N-C′-C_α-C_β and C′-C_α-C_β-S, respectively) rounded to ten are given for the reference ([Mpa^1])-compound in the ECEPP/2 force field.

[b] A dash indicates either that the conformation was above the relative energy limit for the [Mpa^1]-analog in a given force field or, in the case of the calculations on the substituted analogs in the AMBER force field, entirely changed the type of backbone folding (i.e. the RMS deviation from the corresponding conformation of the [Mpa^1]-compound was 1 Å or greater), this corresponding to an entire change of the type of backbone folding.

[c] The energy value in square brackets in the case of the AMBER force field indicates that although the energy value does not change greatly on substitution, a considerable change of geometry takes place (from 0.6 to 1.0 Å), so that the conformation can no longer be regarded as similar to that of the [Mpa^1]-compound, although the type of backbone folding is basically conserved.

[d] Corresponds to conformation βIII(1) of Ref. 3.

[e] Corresponds to conformation βIII(2) of Ref. 3.

[f] Corresponds to conformation βII(1) of Ref. 3 and to conformation 1b (2a) of 1XY and 2XY crystal structures of [Mpa^1]-OT [12].

[g] Corresponds to conformation 1a (2b) of 1XY and 2XY crystal structures of [Mpa^1]-OT [12].

[h] Corresponds to conformation βII(2) of Ref. 3.

[i] Corresponds to conformation βIII′(2) of Ref. 3.

TABLE 3
LOW-ENERGY CONFORMATIONS OF [Mpa[1]]-SUBSTITUTED CYCLIC PART OF OXYTOCIN AND VASOPRESSIN – ECEPP/2 FORCE-FIELD RESULTS

Residue, angle[a]		Type of conformation[b]												
		βIII(1)	βIII(2)	βII(1)	βII(2)	βIII(3)	βII(3)	βIII′(1)	βII(4)	βII(5)	βIII(4)	βII(6)	βII(7)	βII(8)
		Relative energy (kcal/mol)												
		0.0	0.1	0.8	1.3	1.6	2.0	2.6	2.6	2.7	3.4	3.5	3.6	3.8
Mpa[1]	ψ′	−112	−90	−133	78	−60	63	−73	123	−110	−95	140	87	97
	χ′	60	143	58	−159	−53	56	−174	−60	148	61	−55	−151	−66
	χ^2	87	−127	81	144	174	−179	−133	−94	−114	96	−74	73	−111
	χ^3	−113	77	−99	−76	−77	72	104	102	70	−79	103	94	76
Ala[2]	φ	−142	−137	−140	−135	−126	−152	−144	−140	−145	−103	−144	−138	−154
	ψ	168	170	177	178	166	172	130	−177	−179	161	176	−179	176
Ala[3]	φ	−67	−69	−57	−60	−69	−68	56	−63	−58	−67	−61	−60	−64
	ψ	−29	−27	125	98	−24	97	39	96	120	−29	102	98	122
Ala[4]	φ	−75	−72	62	56	−63	57	62	58	59	−70	55	56	58
	ψ	−45	−45	25	38	−43	37	26	34	30	−59	39	39	38
Ala[5]	φ	−152	−154	−159	−163	−156	−164	−126	−168	−154	−169	−160	−163	−153
	ψ	140	146	68	162	132	171	118	166	61	159	174	167	135
Cys[6]	φ	−149	−163	−157	−156	−150	−161	−97	−169	−144	−158	61	−146	51
	ψ	78	86	85	85	81	85	143	87	87	81	84	86	76
	χ^1	−173	177	−173	−174	−169	−168	−59	−174	−177	51	175	−85	−43
	χ^2	117	59	133	110	109	61	−75	69	63	−126	−164	−94	104
	χ^3	−113	77	−99	−76	−77	72	104	102	70	−79	103	94	76

[a] IUPAC-recommended symbols of the peptide dihedral angles are used. In the case of the first residue, due to the absence of the α-amino group the φ angle is absent and ψ′ and χ′ denote the N–C′–C^{α}–C^{β} and C′–C^{α}–C^{β}–S angles, respectively, as in Table 2.

[b] The designation of the type of conformation and conformation numbering system within a given type is the same as in Table 2.

[Mpa[1]] model compound. In the cases where the two procedures gave substantially different final low-energy conformations, the results obtained in one force field were used as starting point for the second force-field calculation, and the cycle repeated until satisfactory 'self-consistency' of the two minimization procedures was achieved.

As mentioned in the previous section, in order to estimate the influence of different side-chain models on the relative AMBER energies, for the [Mpa[1]]-compound we minimized the energy of the resulting conformations in a poly-alanine model (i.e. substituting methyl groups for side chains of residues 2–5). The resulting relative energies did not change more than 0.5 kcal/mol for the low-energy conformations (i.e. within 10 kcal/mol above the lowest-energy conformation).

TABLE 3
(continued)

Type of conformation[b]												
βII(9)	βII(10)	βIII(5)	βIII(6)	βII(11)	βIII(7)	βIII′(2)	βIII′(3)	βII(12)	βIII′(4)	βII(13)	βII(14)	βIII′(5)
Relative energy (kcal/mol)												
4.3	4.4	5.6	5.8	6.1	6.4	6.6	7.1	7.2	8.0	9.0	9.2	9.4
−95	−69	−117	−58	77	76	−101	−143	81	67	−118	−98	−173
63	174	49	−52	−169	−138	69	62	−167	−178	56	59	170
100	−51	45	121	108	151	138	42	67	63	36	134	−111
−84	−63	65	84	−89	−56	−70	66	62	100	73	−77	63
−87	−138	−140	−129	−161	−148	−146	−153	−155	−136	−136	−98	−127
179	178	175	167	−179	162	138	147	164	125	−178	176	142
−62	−60	−61	−65	−61	−76	58	58	−64	55	−54	−57	55
96	110	−30	−23	126	−34	38	40	122	37	110	106	43
57	57	−67	−60	58	−77	60	58	62	63	61	59	69
41	36	−52	−46	37	−41	29	33	25	23	33	36	17
−157	−163	−162	−161	−153	−152	−131	−132	−158	−128	−157	−160	−96
106	164	152	140	110	156	110	102	95	131	84	95	70
−169	−164	−136	−134	66	61	−107	−135	55	−113	−137	−98	−136
84	85	85	82	142	82	142	141	93	133	86	122	89
46	−164	−61	−69	−45	−170	−47	−48	161	−73	−58	−51	−164
−111	125	−128	−96	160	−80	−37	−134	−151	−81	−132	−35	71
−84	−63	65	84	−89	−56	−70	66	62	100	73	−77	63

Only for conformations very high in energy did we observe greater changes (i.e. of several kcal/mol).

After the conformational calculations had been accomplished for the [Mpa[1]]-compound, the conformations of ECEPP/2 or AMBER energy within 10 kcal/mol above the lowest-energy conformations were selected and used as starting points for the calculations on the remaining three compounds.

An analysis of the conformations obtained. Comparison with the results of earlier calculations and with the crystal structure

The relative energies obtained of the conformations of the four compounds studied, using the procedure outlined in the preceding subsection, are summarized in Table 2. The conformations are divided into three classes, depending on the type of the β-turn at residues 3–4 (see the preceding subsection). To complete the qualitative description, the chirality of the disulfide bridge and the approximate (rounded to ten) values of ψ_1 (N–C′–C^{α}–C^{β}) and χ_1 (C′–C^{α}–C^{β}–S) angles are

also included in Table 2. The values of dihedral angles obtained in the ECEPP/2 force field for the reference [Mpa^1]-compound are shown in Table 3.

In order to compare the ECEPP/2 and AMBER results, we first calculated the RMS deviation (at the best superposition of the backbone (N, C′, and C$^\alpha$) atoms and the C$^\beta$ and S atoms of the disulfide bridge) between the ECEPP/2 and AMBER conformations of the [Mpa^1]-compound. The results are shown in the first column of Table 4. The RMS deviations rarely exceed 0.5 Å, indicating that the two force fields produce comparable conformations.

The comparison of ECEPP/2 and AMBER relative energies shows that some correlation exists between them, the overall explained variance being about 30%. The correlation does not improve for the AMBER relative energies calculated in the poly-alanine model; this fact indicates once again that the dimensions of side chains in positions 2–5 do not influence the results significantly. The estimated value of the standard deviation between the ECEPP/2 and AMBER energy is σ_E = 2.5 kcal/mol and there are only a few cases in Table 2 where the difference in relative energy exceeds $2\sigma_E$ = 5.0 kcal/mol, this being the estimated length of the energy uncertainty interval. Generally, the discrepancy increases for higher relative energies. However, when considering the [Mpa^1]-compound, it can be noted that the AMBER counterparts of some low-energy ECEPP/2 conformations are definitely higher in energy. This situation is most pronounced for the βIII(4) conformation (Table 2). A closer inspection of these conformations and the atom-atom contributions to energy revealed that they have a distinctively close contact between the carbonyl carbon and sulfur lone pairs of Cys^6. Because all these sites bear a large negative charge, this results in increased electrostatic repulsion between the carbonyl oxygen and sulfur lone pairs. The unfavorable orientation cannot be changed by rotation of the terminal segment, because the other orientations of this segment with respect to the disulfide bridge lead to nonbonded repulsion between the C-terminal methyl groups and the bridge. In ECEPP/2 the charge distribution of the sulfur atom is approximated by a small single point charge and therefore the electrostatic repulsion does not have much effect on the energy.

In the case of the substituted analogs, it can be noted that some of the ECEPP/2 relative energies are much higher than their AMBER counterparts. However, as shown in Table 4, in these cases minimization in the AMBER force field led to conformations remarkably different from the starting ones (i.e., the RMS deviation between main-chain atoms increased to 0.6–1.0 Å), changing even the type of backbone folding (for conformations with RMS deviation of the order of 1.0 Å). Therefore they can no longer be considered similar to the corresponding conformations of the [Mpa^1]-compound. In the case of ECEPP/2 calculations the substituted-analog conformations were always similar to those of the reference compound.

Two lowest-energy conformations of the [Cpp^1]-compound found in the present extensive analysis (conformations βIII(1) and βII(1) in Tables 2 and 3) are the same as those found for the cyclic part of [Cpp^1,Sar^7,Arg^8]VP [3]. There is also correspondence between other conformations found in this study and those found in a previous one (see footnotes e–i of Table 2), although the energy relations, being qualitatively similar, are not exactly the same. The last fact arises mainly because different values of ε and different side-chain representations were used. It should be noted that in our previous study [3] NMR data were applied extensively in the search for favorable solution conformations (i.e. some of the disulfide-bridge degrees of freedom were also restricted), while in the present study the conformational possibilities of the disulfide bridge were explored more thoroughly. Therefore the above correspondence between the lowest-energy con-

TABLE 4
RMS DEVIATIONS OF MAIN-CHAIN ATOMS OF OXYTOCIN/VASOPRESSIN ANALOGS SUBSTITUTED AT POSITION 1, COMPARED TO THE REFERENCE LOW-ENERGY CONFORMATIONS OF [Mpa^1]-ANALOG OBTAINED IN THE ECEPP/2 (LEFT) AND AMBER (RIGHT) FORCE FIELDS

Type of conformation[a]	Bridge chirality	RMS (Å)[b]						
		Mpa^1	Dmp^1		Cpp^1		α-Dmp^1	
βIII (βI)								
1	L	0.43	0.04	0.05	0.04	0.06	0.19	0.28
2	R	0.37	0.19	0.32	0.21	0.33	0.38	0.08
3	L	0.49	0.35	1.02	0.22	1.00	0.00	0.02
4	L	0.44	0.06	1.04	0.08	1.18	0.18	1.06
5	R	0.41	0.05	0.03	0.07	0.03	0.19	0.21
6	R	0.61	0.39	0.29	0.35	0.81	0.00	0.03
7	L	0.64	0.51	–	0.52	–	0.07	–
8	R	0.64	–	0.12	–	0.14	–	0 18
9	L	–	–	0.05	–	0.05	–	0.65
βII								
1	L	0.28	0.07	0.04	0.08	0.05	0.25	0.30
2	L	0.27	0.23	0.50	0.25	0.48	0.11	0.50
3	R	0.24	0.15	0.10	0.10	0.14	0.00	0.03
4	R	0.15	0.04	0.07	0.05	0.06	0.11	0.07
5	R	0.42	0.08	0.34	0.67	0.34	0.39	0.07
6	R	0.20	0.05	0.05	0.06	0.05	0.16	0.14
7	R	0.26	0.17	0.17	0.17	0.32	0.18	0.11
8	R	–	0.05	–	0.04	–	0.24	–
9	L	0.27	0.05	0.05	0.05	0.04	0.17	0.19
10	L	0.24	0.17	0.06	0.17	0.07	0.18	0.18
11	L	–	0.16	–	0.16	–	0.16	–
12	R	0.27	0.13	0.11	0.14	0.12	0.19	0.22
13	R	0.32	0.12	0.03	0.12	0.03	0.18	0 22
14	L	0.19	0.13	0.07	0.07	0.06	0.17	0.11
15	L	–	–	0.07	–	0.06	–	0.24
βIII′ (βI′)								
1	R	0.20	0.24	0.77	0.24	0.76	0.16	0.81
2	L	0.59	0.07	0.10	0.19	0.08	0.20	0.46
3	R	0.55	0.24	0.06	0.24	0.05	0.32	0.45
4	R	0.23	0.20	0.88	0.21	0.16	0.21	0.62
5	R	0.39	0.14	0.23	0.84	0.71	0.27	0.77
6	R	–	–	0.06	–	0.06	–	0.18

[a] Designation of conformations as in Table 2.

[b] Residual mean square deviation at the best superposition of backbone (i.e. C^{α}, C′, and N) and disulfide-bridge atoms: for Mpa the values are the deviations between ECEPP/2 and AMBER conformations, for the remaining compounds the deviations between the conformations of the substituted and reference [Mpa^1]-compound were computed.

formations of the [Cpp[1]]-compound and the most probable solution conformations of [Cpp[1],Sar[7],Arg[8]]VP validates the results of both studies.

As previously [3], the conformations of βI′/βIII′-type are relatively high in energy, when compared with those of βI/βIII- and βII-type. Even for the [Mpa[1]]-compound there is only one conformation (βIII′; see Table 2) which has a low energy, but only in the ECEPP/2 force field. Because the corresponding AMBER energy is relatively high, owing to the above-mentioned electrostatic repulsion between the cysteine carbonyl oxygen and sulfur lone pairs, this conformation need not be, however, a probable one. Therefore our earlier conclusion [3], that the cyclic part of [Cpp[1]]-substituted oxytocin and vasopressin is in a dynamic equilibrium between the βI/βIII- and βII-type conformations, is now confirmed by a more extensive search of the bridge conformational space and can also be generalized to other, not only [Cpp[1]], compounds.

Two conformations, both with the type II β-turn at residues 3 and 4, have been found in the crystal structure of [Mpa[1]]OT [21] (structures 1XY1 and 1XY2). Both conformers found in the crystal state have their counterparts among the βII-type low-energy conformations of Tables 2 and 3. Conformer 1b (2a), with a left-handed disulfide bridge, is equivalent to the βII(1) conformation, while conformer 1a (2b), with a right-handed disulfide bridge, is equivalent to the βII(5) conformation (the number indicates one of the two pairs of molecules present in the crystal structure and the letter a or b refers to the specific molecule in a pair). Both conformations are definitely low in energy. The RMS deviation of all heavy atoms of the backbone, C^{β}, and disulfide bridge is about 0.3 Å in both cases, indicating very good agreement between the crystal structure and the calculated conformations. This is also shown in Figs. 3a and 3b where each of the two conformations is superimposed onto its crystal counterpart. The good agreement validates the assumption inherent in our previous paper [3] and in this work, that the conformations of the more rigid cyclic part of OT and VP are largely independent of the presence of the more flexible acyclic tail.

It should be noted that, while the crystal-like structure with the left-handed bridge was already found in our previous work [3], the right-handed bridge was found only in this study during the extensive search for possible bridge conformations. Many other low-energy conformations found in this study that differ in the disulfide-bridge geometry also do not have their counterparts among the conformations found in previous studies [3,11,12]. This shows the usefulness of our new bridge-closure algorithm as a tool to explore the conformational space of the disulfide bridge.

Influence of substitution on conformational space. Estimation of possible binding conformations

The agreement between the low-energy conformations obtained in this study and the structures found in the crystal state [21] allows us to conclude that the sets of conformations presented in Table 2 include the most probable types of backbone and disulfide-bridge conformations accessible to the OT/VP ring in rather diverse environments. Therefore, based on these sets of conformations we can analyze the influence of substituents in position 1 on the energy preferences of the disulfide bridge and make an attempt at selecting the putative receptor-bound conformations of the active OT/VP analogs. It could be expected that the changes in the relative energies of the substituted compounds with respect to the corresponding conformations of the reference ([Mpa[1]]) compound result directly from the influence of substitution on the local interactions within residue 1. The (ψ′, χ′)-maps of the C-terminally blocked Mpa, Dmp, Cpp, and α-Dmp residues calculated with the ECEPP/2 potentials are shown in Figs. 4a and 4d. The comparison of the

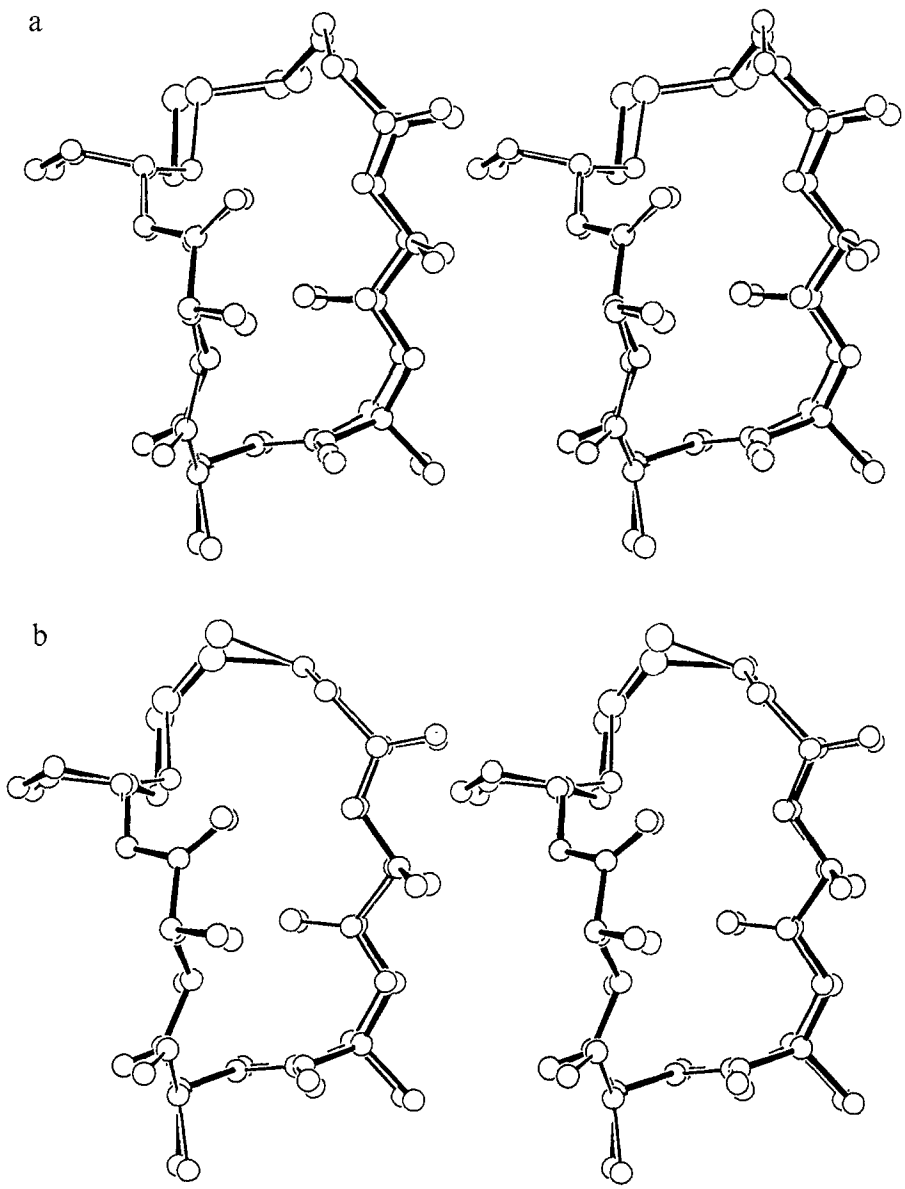

Fig. 3. Superposition of the non-hydrogen backbone, C^{β}, and disulfide-bridge atoms of conformations βII(1) (a) and βII(5) (b) (thin lines) onto conformations 1b (a) and 1a (b) of the 1XY1 crystal structure of the cyclic part of [Mpa^1]-OT.

maps shows that the β-substitution confines the allowed χ'_1 angle values of the Dmp and Cpp residues to three very narrow regions around ± 60° and 180°. Moreover, the angle ψ'_1, although not so restricted, prefers to assume values around ± 100° (however, the tolerance is greater than that for χ'_1 and only the values from the interval [−60°,60°] and around 180° are not allowed). This gives six comparatively narrow regions of favorable local interactions, around $(\psi'_1, \chi'_1) \in$ {(−100°,−60°), (−100°,60°), (−100°,180°), (100°,−60°), (100°,60°), (100°,180°)}. However, as shown in Table 2, the low-energy conformations of the β-substituted compounds do not assume

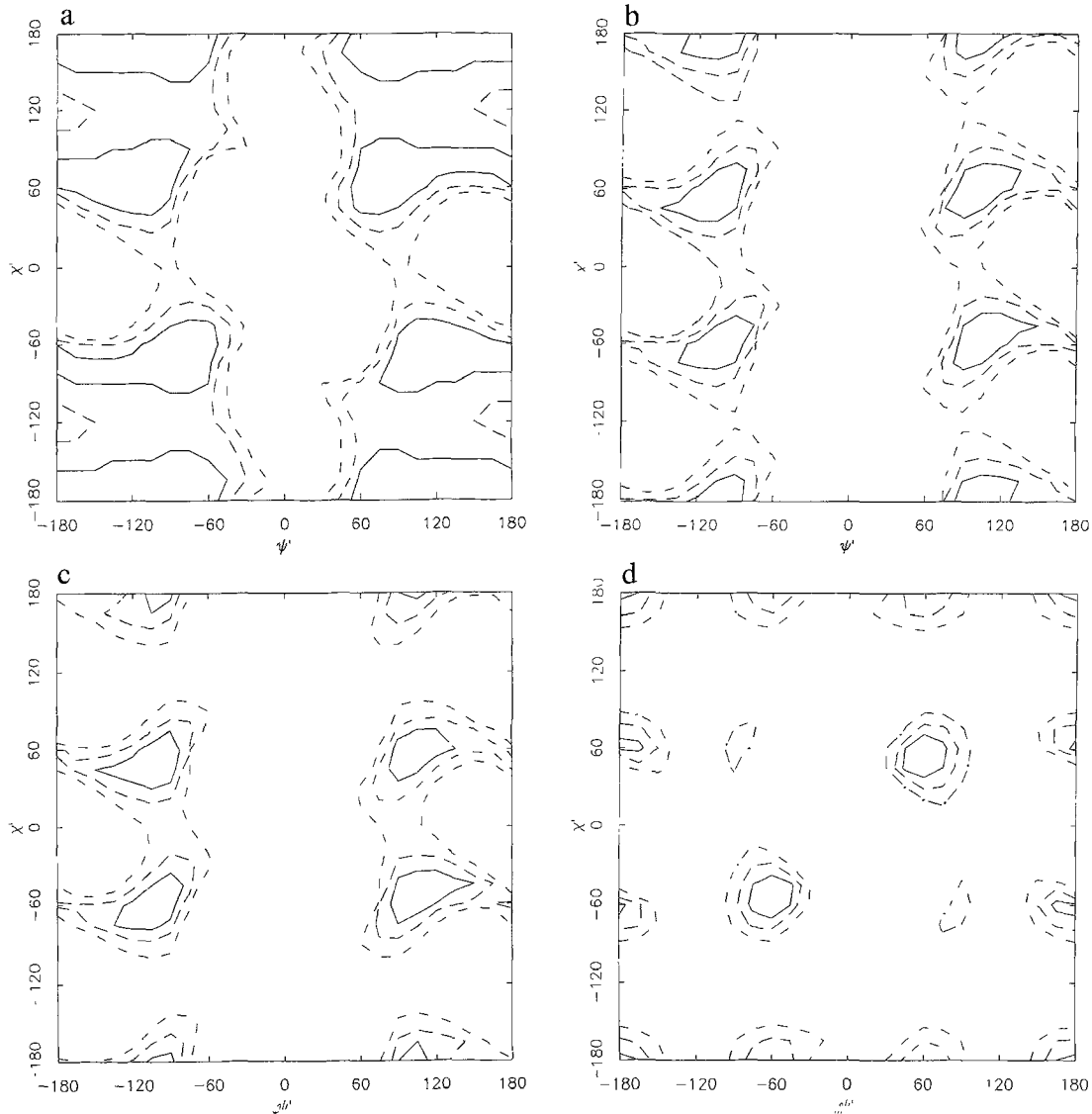

Fig. 4. ECEPP/2 relative-energy maps of the X-NHMe models of the derivatives of cysteine residues studied, with X = Mpa (a), Dmp (b), Cpp (c) and α-Dmp (d). The designation of contours is as follows: solid lines: 2 kcal/mol; dashed lines: 5 kcal/mol; centered lines: 10 kcal/mol.

all these values of the ψ'_1 and χ'_1 angles, but rather the values around (−100°,60°) and (100°,−60°). The exclusion of χ'_1 around 180° can easily be explained, because this value implies steric overlap of the β-substituent with the 20-membered ring. From the remaining four pairs of angles, those with equal signs of ψ'_1 and χ'_1 do not occur for the reference compound, owing to bridge-closure restrictions. For these reasons we can conclude that favorable local interactions within residue 1 are a necessary, but not sufficient condition to determine the allowed conformations of the β-substituted OT/VP ring.

On the other hand, it should be noted that the local interactions within residue 1 determine very accurately the allowed conformations of the [α-Dmp[1]]-compound. In this case the energy map resembles that of the blocked α-aminoisobutyric acid (Aib) residue [22] and the allowed conformational space is severely restricted, with the only allowed ψ′-angle values around ± 60° and 180° (Fig. 4d). In fact, Table 3 shows that conformations with these values of the ψ'_1 angle are little influenced by substitution, while all the other values of this angle lead to a substantial energy increase. It is worth noting that the values of ψ'_1, which result in low-energy conformations of the [α-Dmp[1]]-compound, lead to high-energy conformations of the β-substituted compounds, leaving no conformation which is low in energy for both types of compounds. This could explain the very low activity of the [α-Dmp[1]]-analogs (Table 1).

The different features of both force fields and modes of geometry optimization used in this study are manifested once again in the analysis of substitution influence on the conformational space of the OT/VP cyclic part. Generally, the energy increase is greater in ECEPP/2 calculations. This difference is particularly pronounced for the [α-Dmp[1]]-compound. It is of the same nature as that which places the C^7_{ax} conformation of the blocked alanine about 7.3 kcal/mol above the C^7_{eq} one in the ECEPP/2, but only 0.8 kcal/mol in the AMBER force field [8]. The source of this difference is the use of flexible valence geometry in AMBER which allows for the removal of steric overlap, at the expense of slight distortion of some valence angles [8].

It was suggested by Hruby et al. [2] that a favorable orientation of the bulky β-substituents occurs for the disulfide bridge with a fixed chirality. As shown in Table 3, as a matter of fact, most of the conformations of the reference and the β-substituted compounds with an ECEPP/2 energy within 5 kcal/mol above the lowest-energy one have the left chirality of the disulfide bridge. There is only one conformation (βII(6)) low in energy for all of the β-substituted compounds which has the right-handed bridge chirality. However, it is still higher in energy than the lowest-energy conformation with the left-handed bridge. Most of the conformations with the right-handed bridge, including the βII(5) conformation close to the second crystal conformer of [Mpa[1]]OT, have a relative energy considerably increased on substitution. However, this is a direct consequence of the fact that the right-bridge chirality implies, in almost all of the cases considered, χ'_1 and ψ'_1 angles which are forbidden for the β-substitution. Thus, the statement about the favorable bridge geometry can now be formulated more precisely in terms of the allowed values of the angles χ'_1 and ψ'_1 (see above).

The comparison of the low-energy conformations common for the reference compound and its β-substituted analogs allows us to estimate the possible binding conformations of the OT/VP cyclic part. Because the β-substitution results in strong antagonists, it can be assumed that such analogs have a similar binding conformation as that of the [Mpa[1]]-compound.

In order to determine the set of the most probable binding conformations, we required that the conformations of both the reference compound and the β-substituted analogs have relative ECEPP/2 energies within a common cut-off value. The cut-off was chosen as the length of the estimated energy uncertainty interval which is, according to our previous considerations, 5 kcal/mol. Therefore, we regard the chosen cut-off value as a margin of error of our estimated energies, rather than as that corresponding to Boltzmann-weight cut-off.

First of all, it should be noted that there is no conformation of the βI′/βIII′-type which would satisfy the 5 kcal/mol cut-off criterion for all of the three active compounds. Therefore, the βI′/βIII′-type of backbone structure can hardly be considered as a probable binding conforma-

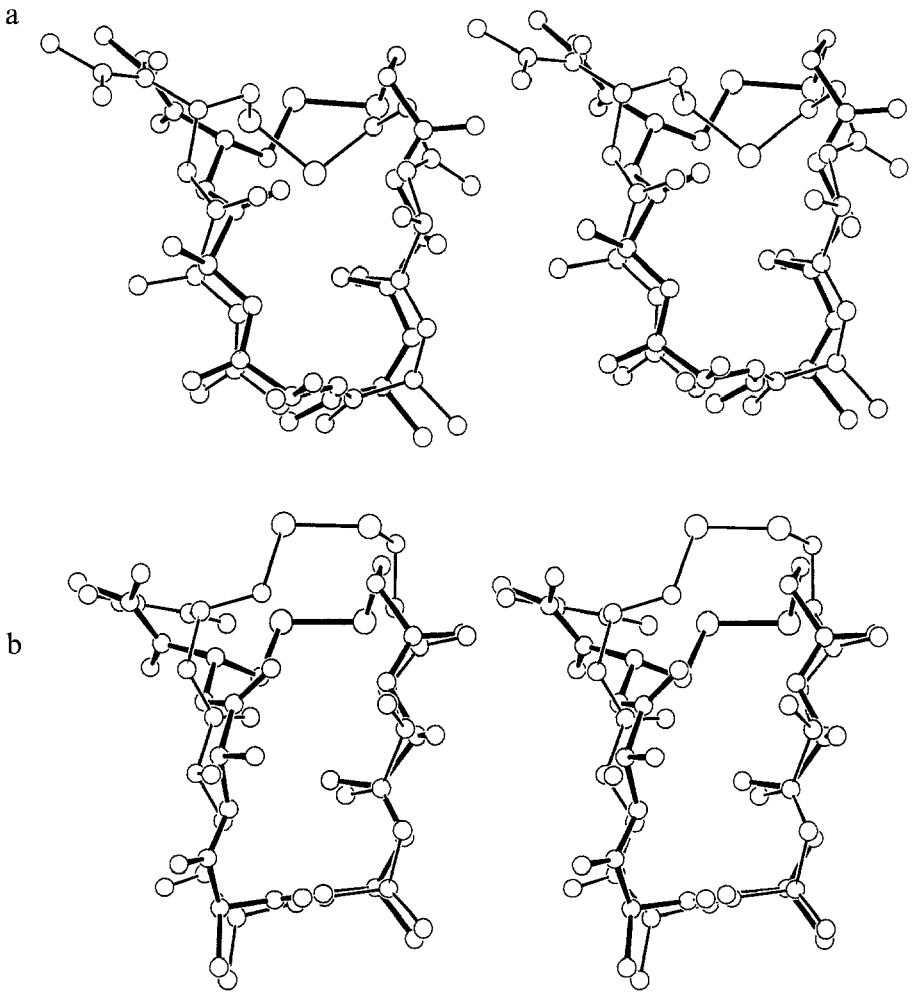

Fig. 5. The putative binding conformations of the cyclic part of OT/VP: (a) βIII(1) (thick lines) superimposed on βIII(4) (thin lines); (b) βII(1) (thick lines) superimposed on βII(6) (thin lines).

tion of the OT/VP analogs. This conclusion is in agreement with our previous study [3], where this type of structure was ruled out based on NMR data.

There are four conformations which satisfy the cut-off criterion: βIII(1), βIII(4), βII(1), and βII(6). The conformations βIII(1) and βII(1) have a very similar bridge geometry, while the remaining two represent different geometries of the bridge. This is illustrated in Figs. 5a and 5b, in which the probable binding conformations of the [Mpa^1]-compound are superimposed (each type of backbone separately). Taking into account our earlier considerations, the βIII(4) conformation should be rejected, as it has a high AMBER energy. This also holds for the βII(9) which has a bridge conformation similar to that of βIII(4) and exceeds the selected cut-off criterion only slightly for the [Cpp^1]-compound. Therefore, most probably, there are only three types of possible binding conformations with regard to the geometry of the 20-membered ring: βIII(1), βII(1), and βII(6). The first two, with a left chirality of the bridge, have a similar backbone folding and an almost identical bridge geometry, with the sulfur atoms oriented towards the different side of the

ring than the side chains of residues 2–5. In conformation βII(6), with right chirality of the bridge, the sulfur atoms are oriented towards the same side of the ring as the side chains, which would probably require a different binding mode. It is therefore probable that only one of the two possible types of disulfide-bridge conformations can bind to the receptor. That this is probably the type represented by the βIII(1)-βII(1) pair is strongly supported by the presence of the βII(1) in the crystal phase and by a higher relative energy of the βII(6) conformation for the [Mpa^1]-compound.

ACKNOWLEDGEMENTS

This work was supported by the Polish National Research Council (KBN) under grant number 1981/4/91 and by the Latvian Council of Science under grant number 431.

REFERENCES

1 Gazis, D., In Jošt, K., Lebl, M. and Brtnik, F. (Eds.) CRC Handbook of Neurohypophyseal Hormone Analogs, Vol. 1, Part 1, CRC Press, Boca Raton, FL, 1987, pp. 106–107.
2 Hruby, V.J. and Lebl, M , In Jošt, K., Lebl, M. and Brtnik, F. (Eds.) CRC Handbook of Neurohypophyseal Hormone Analogs, Vol. 1, Part 2, CRC Press, Boca Raton, FL, 1987, pp. 152–155.
3 Shenderovich, M.D., Kasprzykowski, F., Liwo, A., Sekacis, I., Saulitis, J. and Nikiforovich, G.V., Int. J. Pept. Protein Res., 38 (1991) 528.
4 Tarnowska, M., Liwo, A., Grzonka, Z. and Tempczyk, A., In Kuchař, M. (Ed.) QSAR in Design of Bioactive Compounds, Vol. 2, J.R. Prous Science Publishers, Barcelona, 1991, pp. 361–436.
5 Momany, F.A., McGuire, R.F., Burgess, A.W. and Scheraga, H.A., J. Phys. Chem., 79 (1975) 2361.
6 Némethy, G., Pottle, M.S. and Scheraga, H.A., J. Phys. Chem , 87 (1983) 1883.
7 Weiner, S.J., Kollman, P.A., David, A.C., Chandra Singh, U., Ghio, C., Alagona, G., Profeta, S. and Weiner, P., J. Am. Chem. Soc., 106 (1984) 765.
8 Roterman, I.K., Lambert, M.H., Gibson, K.D. and Scheraga, H.A., J. Biomol. Struct. Dyn., 7 (1989) 421.
9 Palmer, K.A. and Scheraga, H.A., J. Comput. Chem., 12 (1990) 505.
10 Liwo, A., Tempczyk, A. and Grzonka, Z., J. Comput.-Aided Mol. Design, 2 (1988) 281.
11 Nikiforovich, G.V., Leonova, V.I., Galaktionov, S.G. and Chipens, G.I., Int. J. Pept. Protein Res., 13 (1979) 363.
12 Spasov, V.Z. and Popov, E.M., Soviet J. Bioorg. Chem., 7 (1981) 263.
13 Dunfield, L.G., Burgess, A.W. and Scheraga, H.A., J. Phys. Chem., 82 (1978) 2609.
14 Gō, N. and Scheraga, H.A., Macromolecules, 3 (1970) 178.
15 Bruccoleri, R.E. and Karplus, M., Macromolecules, 18 (1985) 2767.
16 Bruccoleri, R.E. and Karplus, M., Science, 235 (1987) 458.
17 Palmer, K.A. and Scheraga, H.A., J. Comput. Chem., 13 (1991) 329.
18 Ortega, J.M. and Rheinboldt, W.C., Iterative Solution of Nonlinear Equations in Several Variables, Academic Press, New York, NY, 1970, pp. 183–187.
19 Bhaskaran, R., Chuang, L.-C. and Yu, C., Biopolymers, 32 (1992) 1599.
20 Scheraga, H.A., Biopolymers, 20 (1981) 1877.
21 Wood, S.P., Tickle, I.J., Treherne, A.M., Prits, J.E., Mascarenhas, Y., Li, J.Y., Husoin, J., Cooper, S., Blundell, T.L., Hruby, V.J., Buken, A., Sishman, A.J. and Wyssbrod, H.P., Science, 232 (1986) 633.
22 Prasad, B.V.V. and Balaram, P., CRC Crit. Rev. Biochem., 16 (1984) 307.